Rock Mech Rock Eng (2011) 44:373–377
DOI 10.1007/s00603-010-0117-2

TECHNICAL NOTE

Deformation and Breakage Properties of Crushable Blocky Materials

EnLong Liu

Received: 12 August 2010 / Accepted: 2 September 2010 / Published online: 18 September 2010

Keywords Biaxial tests · Crushable particulate materials · Blocky materials · Breakage mechanism

1 Introduction

Most geological materials encountered in engineering are particulate materials, which are composed of distinct particles interacting with each other and associated voids. Upon loading, the particulates may slide, rotate and crush or break. The deformation and breakage mechanism of particulate materials is complicated and many experimental studies have attempted to characterize this process (see e.g. Rowe 1962; Drescher 1976; Chappell 1979; Oda et al. 1980; Calvetti et al. 1997; Lanier 2001; Wolf et al. 2003; Delenne et al. 2004). Furthermore, some researchers use theoretical and numerical methods to study the failure mechanism of particulate materials (see e.g. McDowell et al. 1996; Anandarajah 2004; Chang and Hicher 2005).

The aforementioned experimental and theoretical studies focused primarily on the microscopic deformation mechanisms such as sliding and rolling or rotations of particulates that occur in stiff materials. Upon loading, however, the particles of an element of soil are crushed or broken (Hardin 1984; Nakata et al. 2001; Bartake and Singh 2007). This, in turn, profoundly affects the strength and stress–strain behavior of the soil elements. Although a few theoretical methods have been employed to study the crushing mechanism of granular materials, the simulation results need to be confirmed using experimental data. To formulate the constitutive model of particulate materials, which can take into account the influence of microstructure deformation mechanisms, tests on crushable blocky materials at the mesoscale were performed and are the basis for this technical note.

We tracked the mesoscopical breakage process of particulate materials. Biaxial compression tests at 0.045, 0.15 and 0.45 MPa lateral stress were performed on an assembly of blocky materials that were crushable. Finally, we comprehensively investigated the deformation mechanism and breakage processes.

2 Test Methods and Procedures

We devised an apparatus that could be axially loaded using a sample cell from a high pressure triaxial equipment, which was laterally loaded by air pressure. Two transparent rigid glass plates were set in parallel 3 cm apart to keep the specimen under biaxial loading conditions. The size of the specimen chamber was 20 cm × 10 cm × 3 cm. During the loading process, a series of pictures was taken to track the breakage processes of the specimens at the mesoscale.

The blocky materials used in the tests consisted of chalk and purified water, which were mixed uniformly together in a mass ratio of 1:1. After the specimens were formed, they were air-dried under identical conditions. The size of the block was 1 cm × 1 cm × 3 cm, the density was 0.92×10^3 kg/m^3, the unconfined compression strength was 2.1 MPa and the tensile strength was 0.525 MPa.

E. Liu (✉)
State Key Laboratory of Hydraulics and Mountain River Engineering, School of Hydraulic and Hydropower Engineering, Sichuan University, Chengdu 610065, People's Republic of China
e-mail: liuenlong@scu.edu.cn

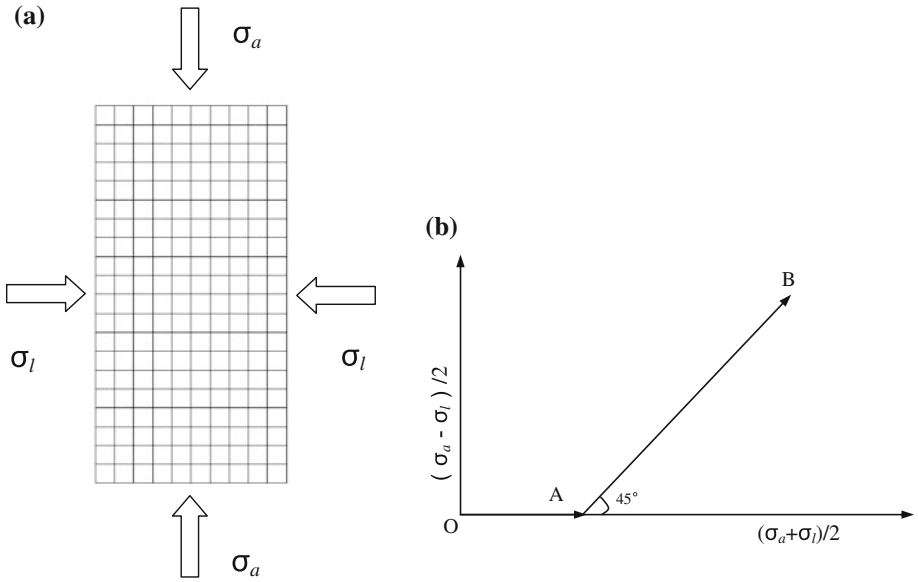

Fig. 1 Pattern of arrangement and stress path: **a** arrangement and **b** stress path

The arrangement of the blocky materials is shown in Fig. 1a. The total number of blocks used for each test was 200. Axial loading was applied by displacement control, and the corresponding loading velocity was set at 0.125 mm/min. During the loading process, the axial displacement and corresponding axial force were recorded by the high pressure triaxial apparatus. The lateral displacements were measured using a micrometer, and the corresponding lateral stress was recorded using a pressure gauge.

The stress path depicted in Fig. 1b was used to carry out the tests. In Fig. 1b, the OA loading stage denotes the axial loads and lateral loads being applied equally, and the AB stage denotes that the lateral pressures remain unchanged while the axial loads are applied until the sample fails. In the following, σ_a,ε_a,σ_l and $\varepsilon_l$represent the axial stress, axial strain, lateral stress and lateral strain, respectively.

3 Test Results and Discussion

3.1 Breakage Processes

Figure 2a–c depicts the breakage processes of the block assembly under the loading stress path presented in Fig. 1b. Three sets of lateral pressure, 0.045, 0.15 and 0.45 MPa, were applied. For each set of lateral pressure, the processes of breakage of the assembly of blocky materials were different as shown in Fig. 2a–c. When the lateral pressure is lower, initially the blocks move toward each other and become closer. At this point, voids appear between blocks, accompanied by cracking of some of them. The breakage bands are formed gradually. Finally, some new blocks crack, leading to additional conjugated breakage bands. When the lateral pressure is high, the blocks move toward each other. Some of the blocks break or are crushed and the breakage bands are formed step by step. The breakage band is formed by shearing under low lateral pressures and by shearing and crushing under high lateral pressures.

3.2 Breakage Modes of the Blocky Materials

Takei et al. (2001) proposed models for breakage modes of chalk bars under one-dimensional compression conditions. For the crushable blocks under biaxial compression presented in Fig. 2a–c, three types of breakage modes are shown in Fig. 3a–c. From the breakage processes presented in Fig. 2, we observe that more of the blocks are vertically split (Breakage Mode A) or failed by shear (Breakage Mode B) when the lateral pressures are low, whereas more blocks are locally crushed (Breakage Mode C) when the lateral pressures are high upon loading. The different breakage modes result from the local stress states of the blocks within the sample. For some samples tested, the three breakage modes A, B and C could be observed simultaneously. Because of differences in loading conditions, the local stresses experienced by individual blocks are different, and thus the blocks fail according to unique breakage modes.

3.3 Stress–Strain Behavior

The stress and strain herein refer to the average stress and the average strain of the specimen consisting of the assembly of blocky materials. Figure 4a, b shows the stress–strain and volumetric strain–axial strain curves for

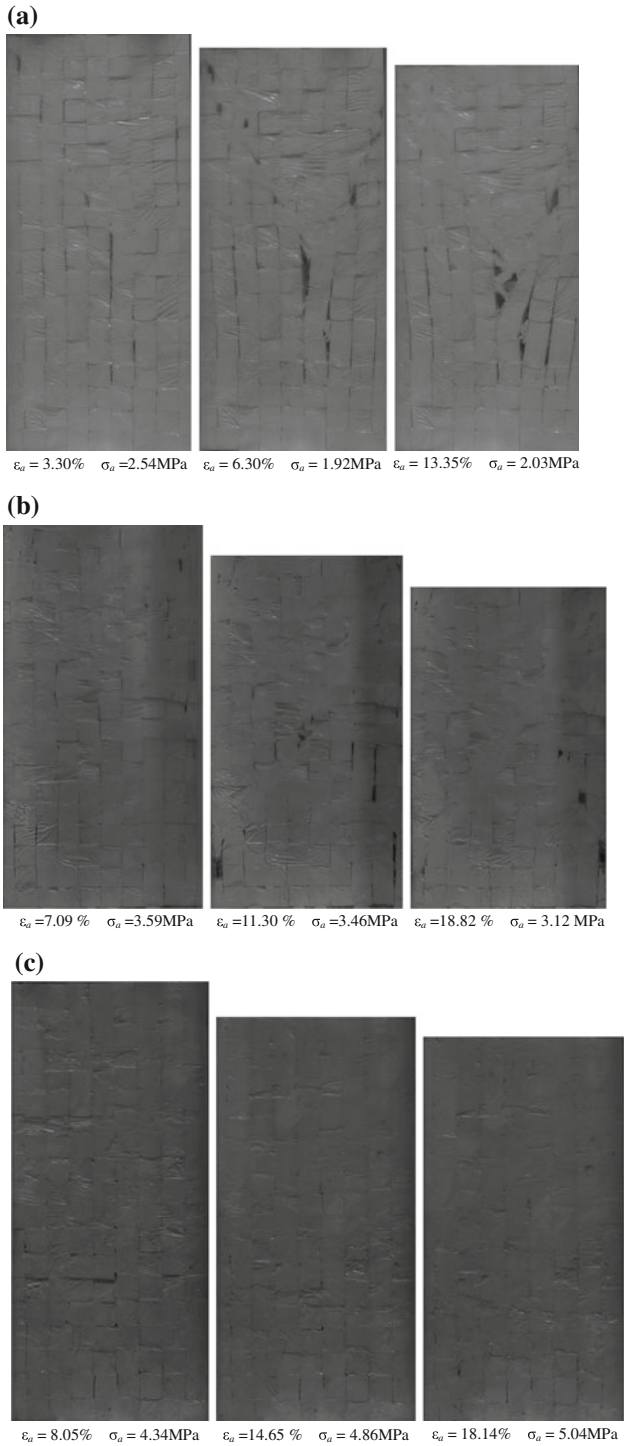

Fig. 2 Breakage processes: **a** $\sigma_1 = 0.045$ MPa, **b** $\sigma_1 = 0.15$ MPa, **c** $\sigma_1 = 0.45$ MPa

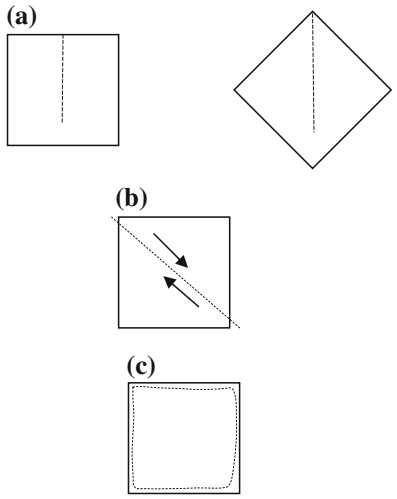

Fig. 3 Breakage modes: **a** breakage mode A (*dashed line* indicates crack resulted by vertically splitting), **b** breakage mode B (*dashed line* slide plane by shear failure) and **c** breakage mode C (*dashed line* indicates the profile of the block after locally crushed)

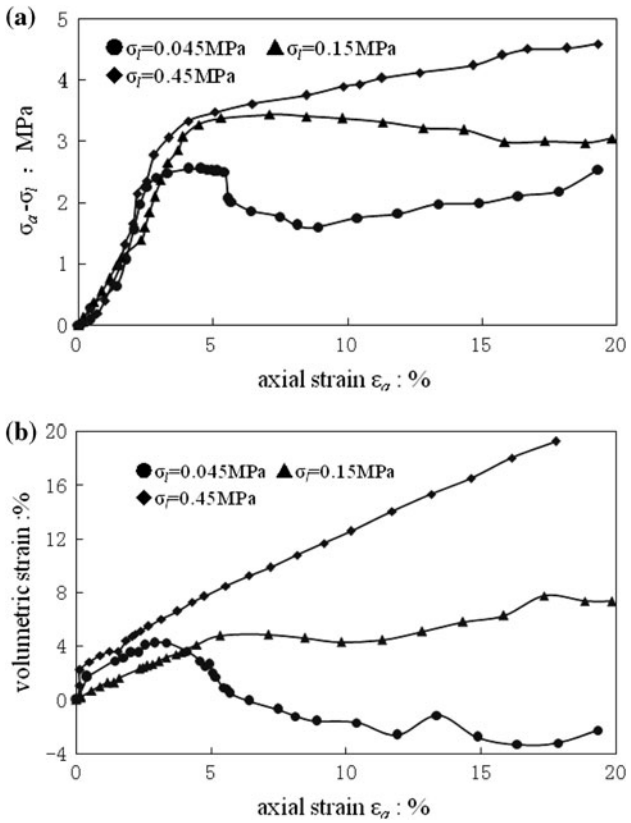

Fig. 4 Strain–stress and axial strain–volumetric strain relationship curves: **a** stress–strain curves and **b** axial strain–volumetric strain curves

tests. Deformational features are summarized as follows: (1) the specimen exhibits strain hardening under low lateral pressure and strain softening under high lateral pressure; and (2) when the lateral pressure is low, the volumetric strain is compressive and then expansive with the increase of axial strain. When the lateral pressure is high, however, the volumetric strain is compressive all the time.

4 Breakage Mechanism Analysis

4.1 Rotation Analysis

During the loading processes, we observed that the blocks slid, rotated and were crushed, because of the different lateral pressures. When the lateral pressures are low, the blocks located along the breakage bands slide, rotate and are crushed (shown in Fig. 5a corresponding to Fig. 2a, which were recorded from another surface of the biaxial compressional apparatus through a transparent rigid glass plate). The other blocks which are located outside of the breakage bands only slide and move closer, having very few rotations. This happens because some of the blocks slide and are split first and then are crushed. This is then accompanied by the emergence of large voids between the blocks under low lateral pressure. The blocks are then able to rotate and form the breakage bands, whereas the other blocks outside of the breakage bands only slide and barely rotate. When the lateral pressures are high, the blocks mainly slide and are crushed, undergoing very few rotations (shown in Fig. 5b corresponding to Fig. 2c). This occurs because many of the blocks slide and are crushed in a manner that forces them to move closer until no room is present between them with high lateral pressure. Finally, the breakage bands, which is wider under low lateral pressure, forms.

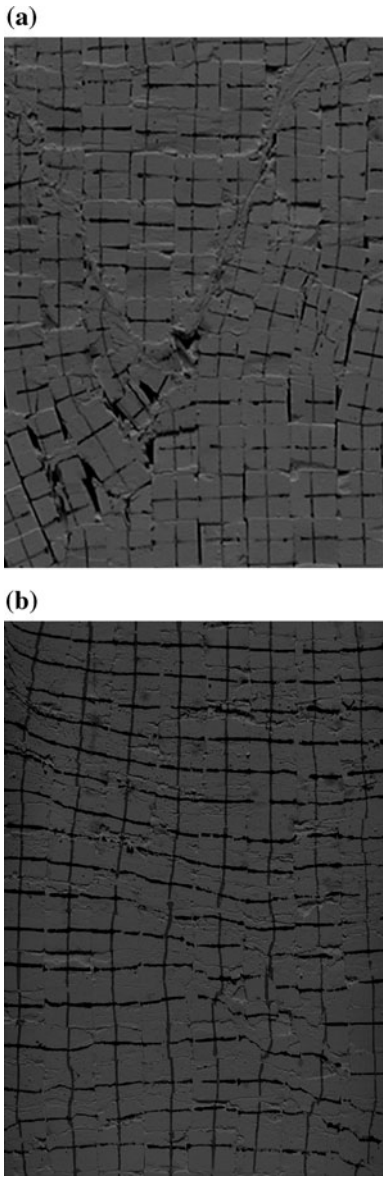

Fig. 5 Slide, rotation and crush (the "+" lines are mutually orthogonal in the *vertical* and *horizontal* directions at the beginning of loading) **a** $\sigma_l = 0.045$ MPa, $\sigma_a = 2.59$ MPa; **b** $\sigma_l = 0.\ 45$ MPa, $\sigma_a = 5.04$ MPa

4.2 Breakage Analysis

Table 1 lists the stress state, axial strain and cumulative crushing ratio of the tested samples corresponding to the breakage processes presented in Fig. 2, respectively. The cumulative crushing ratio (Takei et al. 2001), R_{cc}, is defined as follows:

$$R_{cc} = \frac{n_{cc}}{n_{ALL}}, \tag{1}$$

where n_{cc} is the cumulative number of crushed blocks at each loading stage, and n_{ALL} is equal to 200, which is the total number of blocks in the specimen. The numbers of crushed blocks at each loading stage were visually counted and recorded.

From Table 1, we can conclude that upon loading, the cumulative crushing ratios at failure increase greatly with the increase in lateral pressure. For example (see Table 1), the cumulative crushing ratio at failure is only 14.5% when the lateral stress is 0.045 MPa, whereas it is increased to 88.0% when the lateral stress is 0.45 MPa. This occurs because when the lateral pressure is low, the crushable blocks can easily rotate and slip upon loading. Thus, the energy produced by the external loads is dissipated by the rotation and slip of the blocks, and only a fraction of the energy is dissipated by crushing them.

5 Conclusions

We conclude the following: (1) the blocky materials slide, rotate and are crushed under stress states and, as a result of this process, the breakage bands are formed; (2) the specimens show strain hardening or strain softening due to the loading conditions and stress state, and the volume and lateral deformation are different for each loading stress state; (3) the breakage modes of the blocky materials are

Table 1 Stress state, axial strain and cumulative crushing ratio (%)

Test no. (MPa)	Axial stress, strain and cumulative crushing ratio (%)		
$\sigma_1 = 0.045$	2.54 MPa, 3.30% and (1.5%)	1.92 MPa, 6.30% and (9.5%)	2.03 MPa, 13.35% and (14.5%)
$\sigma_1 = 0.15$	3.59 MPa, 7.09% and (9.0%)	3.46 MPa, 11.30% and (22.5%)	3.12 MPa, 18.82% and (34.0%)
$\sigma_1 = 0.45$	4.34 MPa, 8.05% and (6.0%)	4.86 MPa, 14.65% and (53.5%)	5.04 MPa, 18.14% and (88.0%)

primarily vertically split, with shear failure and local crushing occurring in response to the local stress states induced; (4) upon loading, under lower lateral pressures the blocky materials mainly slide, rotate and are crushed, whereas under higher lateral pressure they primarily slide, are crushed and scarcely rotate.

Acknowledgments The author thanks the anonymous reviewers for their careful review, contributions and critics, which led to the improvement of the manuscript. The author is deeply indebted to Prof. Zhujiang Shen of Tsinghua University and Dr Tielin Chen of Northern Jiaotong University for their valuable discussion and help in performing the tests. This work was funded by The Ministry of Water Resources of the People's Republic of China (Grant No. 200801014) and National Science Foundation of China (Grant No. 90815024 and 51009103).

References

Anandarajah A (2004) Sliding and rolling constitutive theory for granular materials. Earth Space, pp 73–77

Bartake PP, Singh DN (2007) A generalized methodology for determination of crushing strength of granular materials. Geotech Geol Eng 25:203–213

Calvetti F, Combe G, Lanier J (1997) Experimental micromechanical analysis of a 2D granular material: relation between structure evolution and loading path. Mech Cohes Frict Mater 2:121–163

Chang CS, Hicher PY (2005) An elasto-plastic model for granular materials with microstructural consideration. Int J Solids Struct 42:4258–4277

Chappell BA (1979) Deformational response in discontinua. Int J Rock Mech Mining Sci Geomech 16:377–390 Abstract

Delenne JY, Youssoufi MSE, Cherblanc F et al (2004) Mechanical behavior and failure of cohesive granular materials. Int J Numer Anal Methods Geomech 28:1577–1594

Drescher A (1976) An experimental investigation of flow rules for granular materials using optically sensitive glass particles. Geotechnique 26(4):591–601

Hardin BO (1984) Crushing of soil particles. J Geotech Eng 111(10):1176–1192

Lanier L (2001) Micro-mechanisms of deformation in granular materials: experiments and numerical results. In: Vermeer PA et al (eds): LNP 568, pp 163–172

Mcdowell GR, Bolton MD, Robertson D (1996) The fractal crushing of granular materials. Int J Mech Phys Solids 44:2079–2102

Nakata Y, Hyodo M, Hyde AFL et al (2001) Microscopic particle crushing of sand subjected to high pressure one-dimensional compression. Soils Found 41(1):69–82

Oda M, Konishi J, Nemat-Nasser S (1980) Some experimentally based fundamental results on the mechanical behavior of granular materials. Geotechnique 30(4):479–495

Rowe PW (1962) The stress–dilatancy relation for static equilibrium of an assembly of particles in contact. Proc R Soc Lond A 269:500–527

Takei M, Kusakabe O, Hayashi T (2001) Time-dependent behavior of crushable materials in one-dimensional compression tests. Soils Found 41(1):97–121

Wolf H, Kőnig D, Triantafyllidis T (2003) Experimental investigation of shear band patterns in granular material. J Struct Geol 25:1229–1240